NJC

Accepted Manuscript

This article can be cited before page numbers have been issued, to do this please use: Y. Wang, R. Wang, D. Xu, C. Sun, L. Ni, W. Fu, S. Zeng, S. Jiang, Z. Zhang and S. Qiu, *New J. Chem.*, 2016, DOI: 10.1039/C5NJ03387J.

ROYAL SOCIETY OF CHEMISTRY

www.rsc.org/njc

NJC

View Article Online
DOI: 10.1039/C5NJ03387J

PAPER

View Article Online
View Journal

The Synthesis and Properties of MFI Zeolites with Microporous, Mesoporous and Macroporous Hierarchical structures by a Gel-casting Technique

Ying Wang[a], Runwei Wang[a], Diou Xu[a], Chuanyin Sun[a], Ling Ni[a], Weiwei Fu[b], Shangjing Zeng[a], Shang Jiang[a], Zongtao Zhang*[a] and Shilun Qiu*[a]

Received 00th January 20xx,
Accepted 00th January 20xx

DOI: 10.1039/x0xx00000x

www.rsc.org/

The comparatively small micropore dimensions of bulk ZSM-5 zeolites often limit both the adsorption and the catalytic conversion of large organic molecules. Here, we report that the ZSM-5 zeolites were prepared by a gel-casting technique with microporous, mesoporous and macroporous hierarchical structure. The as-prepared samples were characterized by X-ray diffraction (XRD), scanning electron microscopy (SEM), Transmission electron microscopy (TEM), nitrogen adsorption, Temperature-programmed-desorption of ammonia (TPD-NH3) and Fourier Transform Infrared Spectroscopy (FTIR) measurements. The hierarchical structured ZSM-5 zeolites were used to carry out catalytic cracking reaction of 1, 3, 5 - isopropyl benzene and n-hexadecane. Data shows that compared with traditional ZSM-5, Beta or Al-MCM-41, this modified ZSM-5 displayed preferably catalytic activity and selectivity.

Introduction

In general, zeolites are crystalline aluminosilicates with well-defined porous structures in which water and other types of molecules can pass through.[1] Zeolites are widely used in the fields of catalysis, adsorption and separation. However, most of these pores are smaller than 2 nm and the molecules transferring to the active sites locating inside these micropores can be slowed down by diffusion constraints. When different sizes of pores, such as mesoporous or macroporous crystals are present, it is possible to facilitate the transport of bulky molecules in these materials. [2-7]

Among the various of natural and synthetic zeolites, ZSM-5 zeolites are widely used in petrochemistry and chemical industry for series of reactions involving cracking reaction and alkylation reaction.[8] The penetrating and crossing microporous networks, possess straight channels along the b axis (0.53 nm × 0.56 nm) and zigzag channels along the a axis (0.51 nm × 0.55 nm), this structure endows the ZSM-5 with high shape and size selectivity.[9] Hence, ZSM-5 zeolites fail to catalyze larger molecules. Because of their diffusion limitations in the microporous channels and carbon deposition in the porous systems, ZSM-5 zeolites have severe catalyst deactivation.[10] As we all know, construction of ZSM-5 materials with different levels of pores can improve reaction efficiency and minimize channel blocking.[11-14] It may be a good choice to solve the problems.

Producing gasoline by catalytic cracking of petroleum began in about 1912. The early pioneering work was carried out by Eugene Houdry[15]. Catalytic cracking cracks valueless high molecular weight hydrocarbons into more valuable by-products (low molecular weight) like gasoline, LPG Diesel along with very important petrochemical feedstock like propylene, C4 gases like isobutylene, Isobutane, butane and butene. According to the IEA's World Energy Outlook, global energy demand will grow more than a third over the period to 2035, 60% of the increase come from rising living standard of China, India and the Middle East.[16] The impending challenge we are facing with is how to fully crack the heavy residue oil to various valuable chemical products. The pores of the traditional catalyst are too small to prevent the crossing of the large molecules (crude oil and residue), which directly hinders the cracking reactions. We put forward the research basing on a series of environmental and energy problems. To facilitate reactant molecules and products easily to transport to the active sites, efforts have been made to obtain hierarchical porous zeolite materials with micro-, meso- and macro-porosity.[17-26]

[a] College of Chemistry and State Key Laboratory of Inorganic Synthesis and Preparative Chemistry, Jilin University, Changchun 130012, China.
E-mail: sqiu@jlu.edu.cn; Fax: +86 431 85168115; Tel: +86 431 85168115
zzhang@jlu.edu.cn;Fax: +86 431 85168115; Tel: +86 431 85168115
[b] Experimental Center of Shenyang Normal University, Liaoning Shenyang 110034, P. R. China

† Supplementary Information (ESI) available: TG-DTA curves of ZSM-5, A-ZSM-5, G-ZSM-5and calcined G-ZSM-5 and Catalytic Activities in Cracking of 1, 3, 5-Triisopropylbenzene and Hexane on Various Catalysts. See DOI: 10.1039/x0xx00000x

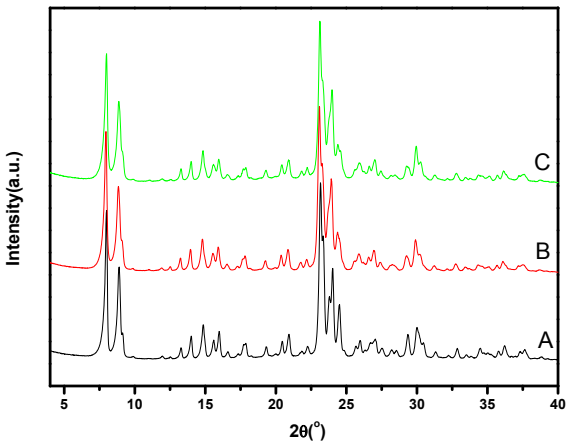

Figure 1. XRD patterns of (A) initial ZSM-5, (B) the ZSM-5 After treating with alkaline (A-ZSM-5), and (C) Gel-casting sample (G-ZSM-5).

Hierarchical zeolites are generally fabricated by post-synthesis treatments, template self-assembly, etching in acid or base solution and so on. Janssen et al.[27] presented an idea on the generation of mesopores in hierarchical zeolites that selects carbon as a template during the synthesis. Wang et al.[28] and Zheng et al.[29]prepared meso-ZSM-5 zeolites during hydrothermal treatment using Beta and Mordenite zeolites as Si/Al source, respectively. Abelló et al.[30] synthesized hierarchical materials by desilication of ZSM-5 zeolites. However, the conversion processes are extremely slow and the final structures are usually composites of the starting materials and the zeolite with non-uniform microstructure.[31] In this paper, hierarchical structured ZSM-5 zeolites with micropores, mesopores and macropores were prepared using a gel-casting technique. The hierarchical structured ZSM-5 zeolites were used to carry out cracking reaction of n-hexadecane and showed higher catalytic activity and selectivity than that of traditional ZSM-5, Beta, Al-MCM-41[32]. Further, the gel-casting method makes G-ZSM-5 possible as technical catalysts. [33,34]

Results and discussion

Hierarchical porous ZSM-5 zeolites were synthesized by hydrothermal synthesis, alkaline-media erosion (A-ZSM-5), gel-casting method and calcined under appropriate temperature(G-ZSM-5). Moreover, the G-ZSM-5 zeolite with excellent properties of catalytic cracking 1, 3, 5- triisopropylbenzene and n-hexadecane were fabricated by this simple method.

Structural properties

The XRD patterns of all of the samples are shown in Figure 1, initial ZSM-5, treated with alkaline (A-ZSM-5) and Gel-casting sample (G-ZSM-5), respectively. Figure 1A shows the X-ray diffraction (XRD) pattern of the as-synthesized initial ZSM-5, exhibiting the typical peaks associated with MFI-type structure with ordered micropores. In Figure 1B, the relative intensities of the typical peak decrease after treating with concentrated alkaline solution. Such decrease can be explained by a partial removal of microporous structure to form some irregular mesopores, these differences also present in Figure 1A and Figure 1C. In Figure 1B and 1C, the diffraction peaks well corresponding to zeolite MFI structure in the wide-angle XRD pattern, indicating that all as synthesized zeolites are still preserved with ordered micropores.

The G-ZSM-5 sample photographs were shown in Figure 2A. The synthetic process is monitored by SEM techniques. According to the SEM images Figure 2B, all of the initial precursors crystals exhibit spheres-like morphology with smooth surface, and the average crystal surface size of individual spheres is about 150-200 nm. The mesopores are created with random morphology (Figure 2C), as evidenced by the decrease relative intensity of diffraction peaks in

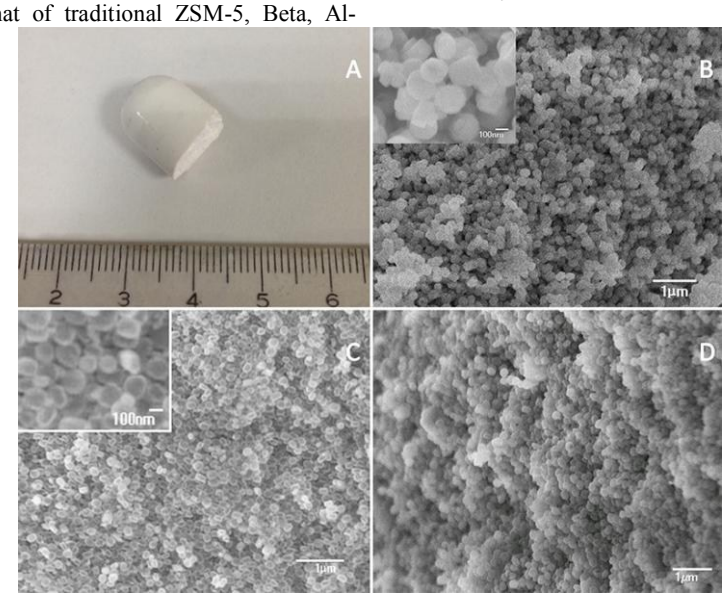

Figure 2. Photograph, SEM images of the sample (A) a photograph of the final sample (taken with a digital camera), (B) ZSM-5, (C) A-ZSM-5, and (D)G-ZSM-5.

View Article Online
DOI: 10.1039/C5NJ03387J

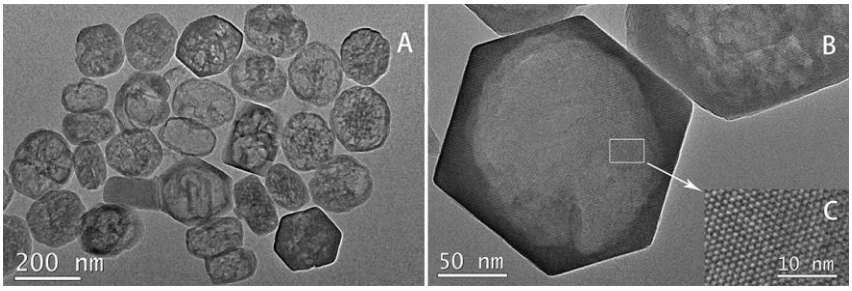

Figure 3. Transmission electron microscopy (TEM) images of ZSM-5 which were treated with gel-casting method(A), (B) and (C) the magnification of a region in A for clarity.

the wide-angle XRD pattern (Figure 1B) due to the erosion in alkaline media. The changes in morphology and crystallinity of the mesoporous walls are observed by TEM (Figure 3). The products obtained over Gel-casting method (Figure2D) retain the well-defined microporous structures and irregular mesopores. On the other hand, random macropores can be clearly seen caused by organic polymers.

TEM (Figure 3) images demonstrate that the hollow structure has well defined hexagon shape and uniform size (150 nm). The TEM image of the zeolite crystal (Figure 3A) displays the mesopores as brighter features pervading the crystal, yet without clear indication of their shapes and sizes, since they are irregular. It is note worthy that the microporous wall can be clearly observed from the high resolution TEM (HRTEM) image (Figure 3C). Due to the grinding and ultrasonic of the samples, the intercrystal macropores can not be observed directly from the TEM images.

Surface properties

The crystallinity of the samples is assessed by the intensity ratio of the vibration band at 550 cm^{-1} over that at 450 cm^{-1} in the FTIR spectroscopy. The existence of the 550 cm^{-1} band can be ascribed to MFI structure typical double five membered rings of T-O-T (T = Si or Al), and the 454 cm^{-1} band corresponded to characteristic bending vibration of T-O. In addition, The IR peaks at 1224, 1095 and 802 cm^{-1}, corresponded to characteristic peaks of the ZSM-5 zeolite frame vibration peak.[35] The band observed at 1224 and 1095 cm^{-1} is assigned to asymmetric stretching vibration of internal tetrahedron structure of ZSM-5 zeolite, and the band at 802 cm^{-1} is similar to symmetric stretching vibration of internal tetrahedron structure. In the Figure 4 there is an additional band of 3446 cm^{-1} which is assigned to O-H of zeolite ZSM-5 or water adsorbents. The FTIR spectrum of A-ZSM-5 is similar to that of ZSM-5, which indicates that the structure of ZSM-5 zeolite is not broken by alkaline erosion. However the band at 1095 cm^{-1} broadened, which should be resulted from low crystallization, due to the consumption of Si in the process of alkaline post-synthesis. As expected, peaks corresponding to the C-C vibration mode of organic polymer are observed in the region of 1421cm^{-1} for as-made G-ZSM-5(C), while no IR signal corresponding to the polymer is detected after calcination at 550ºC. Moreover, The IR peak at 1421$cm^{-1}$is quite weak due to the low percentage of polymer in the sample. However after calcination, the typical band at 1095 cm^{-1} sharpened proving the fact that the crystal becomes smaller and more perfect.

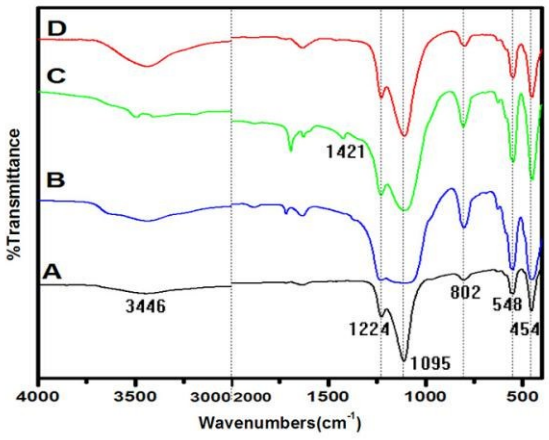

Figure 4. FTIR spectra of (A) ZSM-5, (B)A-ZSM-5, (C) G-ZSM-5 and (D) calcined G-ZSM-5.

Figure 5 shows the N_2 adsorption – desorption isotherms of the resulting ZSM-5 samples. All of the samples exhibit the characteristic Type I adsorption isotherms with a steep increase in the curve at a relative pressure of $10^{-6}<P/P0<0.01$, which is due to the filling of micropores. While a small uptake near saturation pressure in the isotherms of the resulting materials are observed, which indicates that secondary mesopores or macropores are present in the crystals. Apart from the micropores with diameters of about 0.55 nm (Figure inset), which is typical for ZSM-5, samples A-ZSM-5 (Figure 5B) and G-ZSM-5 (Figure 5C) exhibit the type-IV isotherms, and the large hysteresis loops in the region $0.40<P/P_0<0.98$ are observed due to the capillary condensation in the mesopores (Figure 5) which may be of importance for mass transport. Meanwhile, the pore size distribution in 2–100 nm also demonstrate the existence of hierarchical porosity in samples A-ZSM-5 and G-ZSM-5 (Figure 5 inset). The detailed surface area ,Si/Al ratio and pore volume data are summarized in Table 1. Notably, the hierarchical sample A-ZSM-5 displays significantly increased surface (394.15 m^2/ g)

View Article Online
DOI: 10.1039/C5NJ03387J

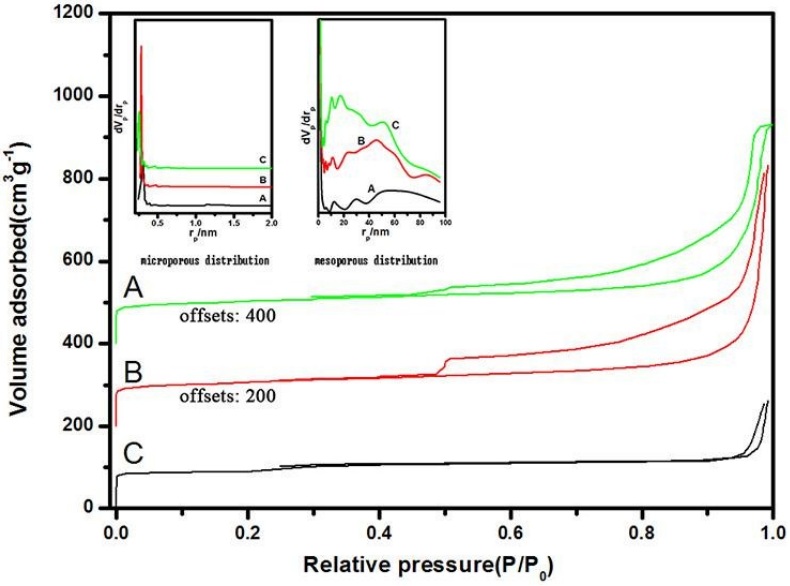

Figure 5. Nitrogen adsorption and desorption isotherm and the microporous and mesoporous distribution for (A)ZSM-5, (B) A-ZSM-5, and (C) G-ZSM-5

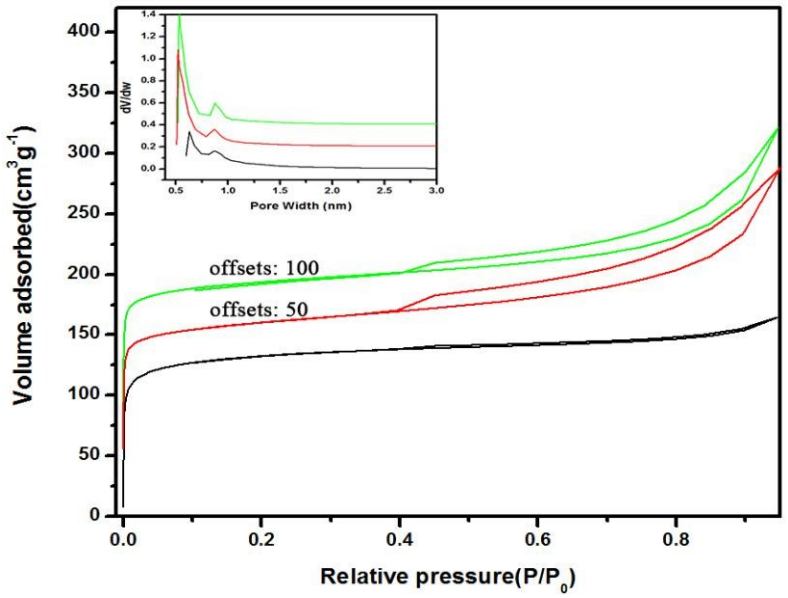

Figure 6. Argon adsorption and desorption isotherm and the microporous and mesoporous distribution for (A) ZSM-5, (B) A-ZSM-5, and (C) G-ZSM-5

and mesopore volume (0.9451 cm^3/g) as compared with the conventional microporous ZSM-5 due to the alkaline erosion with 50% Si/Al ratio reduction. In accordance with the SEM and TEM observations, there are two different levels of pores existing in the hierarchical G-ZSM-5 samples, that is, micrometer sized pores (ca. 1 μm) corresponding to the line channals left by organic moleculars and nanometer-sized mesopores (ca. 40 nm) resulted from a small part of framework silicon lost during the NaOH treatment. Compared with A-ZSM-5, a slightly lower uptake for G-ZSM-5 is expected due to the more compact nanocrystals by adding organic polymers. Argon adsorption - desorption isotherms is as same as N_2 adsorption - desorption isotherm (Figure 6). Compared with nitrogen sorption, it is better to use argon sorption to measure micropores (Figure 6 inset). This is because argon is inert gas and it has little effect on solid surface. The temperature of liquid argon is higher than nitrogen and it is easier to meet the equilibrium time. Argon gas molecular diameter and saturated vapor pressure is low, which can detect a larger range of diameter of porous, so it is reasonable to get a higher result of argon sorption compared with nitrogen sorption.[36] But the actual results of A-ZSM-5 and G-ZSM-5 are different from the theoretical value, which may be causede by the varieties of the porous materials (Table 1).

NJC Paper

View Article Online
DOI: 10.1039/C5NJ03387J

Table 1. Si/Al ratio and derived parameters obtained from the N_2 and Ar physisorption isotherm

sample	[a]BET surface area, (N2) m^2/g	pore vol, cm^3/g	[b]Si/Al ratio	BET surface area, (Ar) m^2/g	t-Plot micropore volume, (N2), cm^2/g	t-Plot micropore volume, (Ar), cm^2/g	t-Plot external surface area, (N2) m^2/g	t-Plot external surface area, (Ar) m^2/g
ZSM-5	358.25	0.38	63.62	398.10	0.09	0.13	171.45	100.16
A-ZSM-5	394.15	0.95	38.30	338.01	0.09	0.10	189.18	106.87
G-ZSM-5	382.27	0.80	38.99	330.11	0.09	0.10	148.02	97.839

[a] The specific surface area calculated using the BET equation.

[b] Si/Al ratio calculated from the ICP.

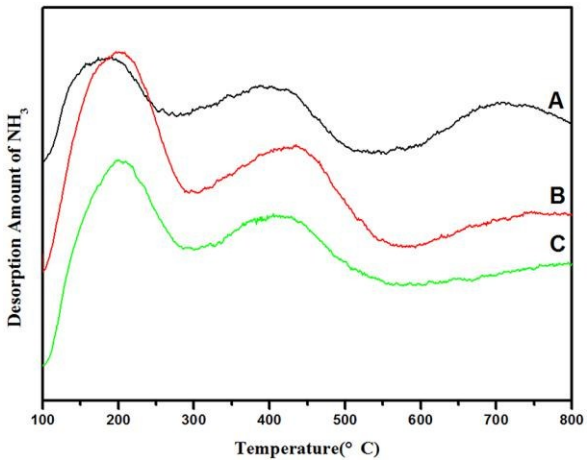

Figure 7. Temperature - programmed desorption of ammonia (NH3-TPD) curves for various samples of (A) ZSM-5, (B) A-ZSM-5, and (C) G-ZSM-5.

Thermal and Catalytic properties.

Supplementary Figure S1 shows TG/DTA curves comparison of the four catalysts. A-ZSM-5, G-ZSM-5 and calcined G-ZSM-5 exhibit similar loss patterns from room temperature to 300 ºC which is the typical of ZSM-5, attributed to the loss of adsorbed water. At 320 ºC to 420 ºC important differences are observed, and the hierarchical porous G-ZSM-5 samples displays more weight loss, the results vary depending on the organic polymers degradation. Until 800 ºC, the overall TG/DTA profiles do not show significant weight loss (around 1 wt%), proving the high thermal stability of G-ZSM-5 compared with ZSM-5. The acidity of the calcined samples is evaluated by NH_3-TPD measurements and the profiles are shown in Figure 7. The desorption temperature indicate the acidic strength, whereas the peak area indicates the acidic concentration of the samples. All the samples show two desorption peaks: the first peak in the range of near 200 ºC corresponds to weak acid sites, which is attributed to T–OH (T = Si, P, Al) hydroxyl groups; the second peak at high temperatures in the range of 380–410 ºC, corresponds to strong acid sites.[38] As indicated in Figure 7, the strong acid strength of samples ZSM-5, A-ZSM-5 and G-ZSM-5 are similar, while the concentration of weak acid sites gradually increases with the decrease of the silicon contents in these nano ZSM-5 samples. Finally, for G-ZSM-5, the peak at about 720 ºC can be ascribed to stronger acid sites. From the conversion of hexane cracking in Supplementary Table 2S, G-ZSM-5 has more Bronsted acid sites than conventional ZSM-5 and MCM-41.

Catalytic cracking activities of 1, 3, 5 triisopropylbenzene over various catalysts are given in Supplementary Table 1S. HZSM-5 is almost inactive due to its relatively small pore size and the large diameter of the molecules to be cracked.[29] HMCM-41 shows high activity under 400 ºC. However, it is completely loses activity after treatment in boiling water for 6 h or at 600 ºC for 2 h.[45] Under 240 ºC, the conversion of the 1, 3, 5-triisopropylbenzene has a sharp decrease, attributing to the cracking temperature below its boiling point, and the liquid molecules cannot be completely gasified. In addition, the yield of propylene in experiment is lower than that in theory, which may ascribe to the coke forming. G-ZSM-5 with micro-, meso- and macro-porous system exhibited catalytic activity as high as that of HMCM-41 under 320 ºC. The catalytic cracking conversion of n-hexadecane remained the same for long cycle life more than 30 times, indicating G-ZSM-5 showed stable catalytic properties. G-ZSM-5 shows the longest catalyst lifetimes of the catalysts studied and higher selectivity of

NJC Paper

View Article Online
DOI: 10.1039/C5NJ03387J

Table 2. Catalytic Activities in Cracking of n-hexadecane on Various Catalysts

catalyst	temperature ℃	conversion, %	Selectivity,%				
			C1-C4	C5-C7	C8	C9-C11	C12-C15
Beta	360	42.58	0.24		96.5		3.27
Beta	320	2.53	5.65	6.35	57.08	13.98	16.94
ZSM-5	360	34.7	1.3		80.5		18.2
ZSM-5	320	0.95	3.47		70.86		25.67
MCM-41	360	2	13.7	2.0		3.4	80.9
SBA-15	360	1.6	10.30	0.19	0.90	0.31	88.30
G-ZSM-5	250	0.70		11.1		88.9	
G-ZSM-5	280	69.9	2.53	2.79	73.37	3.58	17.73
G-ZSM-5	320	89.7	0.31		97.47		2.22
G-ZSM-5	360	98.5	0.20	0.04	98.7	0.09	0.97

[a] The conversion was calculation by internal reference method.

[b] Selectivity=the area of the target product/all the area of the product.

propylene, and suggest that it is a good candidate catalyst for industrial cracking of petroleum.

To further demonstrate the superiority in catalytic application, catalytic tests of n-hexadecane conversion were carried out over our catalysts, a model compound of heavier hydrocarbons. Catalytic cracking of n-hexadecane (Table 2) shows that G-ZSM-5 exhibits a higher activity than that of HZSM-5 and Beta at 360 ºC. The experimental results show that the conversion of n-hexadecane are 1.6 and 2 over SBA-15 and MCM-41 respectively, which further indicate the presence of mesopores is not the only reason for G-ZSM-5. HZSM-5 and Beta exhibit a lower conversion due to their relatively small pore size, and the catalytic cracking of n-hexadecane just takes place at the surface of the catalysts. But the conversion of n-hexadecane on mesoporous materials (MCM-41 and SBA-15) is close to zero which may be related to the strong acidity requirements for this reactive feedstock. Moreover, the G-ZSM-5 catalyst shows the highest catalytic activity among these catalysts and better thermal stability. The various temperature (Table 2) are summarized with G-ZSM-5, ZSM-5 and Beta, and the conversions reduce with the temperature decrease, but the reduction degree of G-ZSM-5 is smaller than others, proving coke formation over the G-ZSM-5 catalyst is not significantly obvious, further indicating higher catalyst stability as the result of its enhanced porosity. It can be widely used in the cracking reaction of n-hexadecane under low temperature. Under 250 ºC, the reaction temperature is lower than its boiling point , and the conversion approaches zero.

The transportation of 1, 3, 5-triisopropylbenzene is heavily hindered by the microporous structure of traditional ZSM-5 and Beta, through the micropores providing unique activity in cracking 1, 3, 5-triisopropylbenzene. Hence, the conversion over that traditional zeolites is much lower than that of mesoporous materials, such as H-MCM-41. The hierarchical G-ZSM-5 zeolites with micro-, meso- and macroporous structures completely overcome the delivery problems of traditional zeolites, and the conversion on G-ZSM-5 is as high as H-MCM-41. The cracking reaction of 1, 3, 5-triisopropylbenzene can occur on weak acid sites, and H-MCM-41 has a relatively high conversion. However, the cracking of n-hexadecane can only take place on strong acid sites, thus, traditional mesoporous materials, such as H-MCM-41 and SBA-15 fail to perform well. The conversions on ordinary zeolites display relatively high, attributing to n-hexadecane with molecular chain conformation having more freedom into the micropore under high temperature. However, the chain flexibility of n-hexadecath decreases once the reaction temperature lower than 360 ºC, which directly reduces the transporting efficiency, directly resulting to the conversion decreased. On the contrary, mesopores and macropores within the G-ZSM-5 are much larger than the molecular size of n-hexadecane. Although under a lower temperature, zeolites G-ZSM-5 containing both micro- and meso- macropores, still shows efficient mass-transport property.

Trimodal Porosity facilitate mass transfer from the surface of the zeolite crystal followed by transport in small mesopores, finally allowing diffusion into short micropores where catalysis takes place. Additionally, the acid sites of G-ZSM-5 have been remarkably increased. Hence ,the typically synthesized G-ZSM-5 with different levels pores shows absolute superiority in catalysis cracking large reactants and products.

Conclusions

Hierarchical structured ZSM-5 zeolites with microporous, mesoporous and macroporous systems were synthesized by using a gel-casting technique. The G-ZSM-5 possessed a relatively large surface area of 382.27m^2/g and exhibited good thermal stability and high acidity. For the cracking of n-hexadecane, G-ZSM-5 displayed good catalytic properties with high activity and selectivity and long catalyst lifetime, when compared to the traditional ZSM-5 , Beta, Al-MCM-41. G-ZSM-5 materials, combination of micropore, mesopore and macropore had advantageous situations for the easy accessibility to all the acid sites and reducing the formation of coke precursor with poor diffusion efficiency highly, additionally, the macroscopic feature and the level of pores can be controlled, so the materials would widely used in residue fcc and hydrocracking macromolecules reactions.

Experimental

1. Materials

Tetrapropylammonium Hydroxide (TPAOH, 25wt % aqueous solution) Tetraethyoxysilane (TEOS), sodium hydroxide (NaOH), Aluminium isopropoxide, N, N-methylenebisacrylamide, ammonium persulfate ($(NH_4)_2S_2O_8$), Ammonium nitrate (NH_4NO_3), acrylamide ($CH_2NCHCONH_2$). All chemicals were commercial samples from Aldrich and used without further purification.

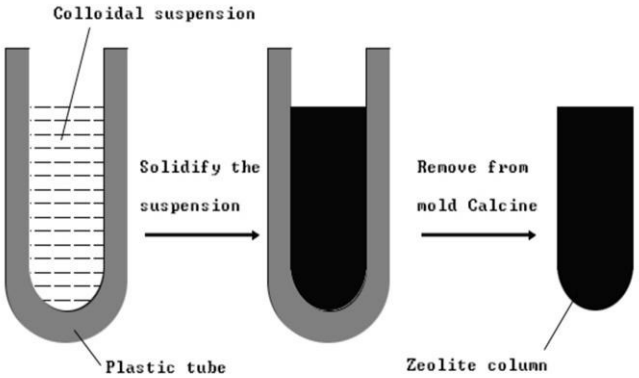

Figure 8. Schematic representation of the gel-casting forming process for a Plastic tube. The colloidal suspension consists of molecular sieve and organic monomer (AM), crosslinker (MBAM), and initiator $(NH_4)_2S_2O_8$.

2. Synthesis.

View Article Online
DOI: 10.1039/C5NJ03387J

Nanoscale zeolite ZSM-5 with size of 100-200 nm as the starting material was hydrothermally synthesized according to a reported method [37]. The mole ratios of the materials were Al_2O_3 / SiO_2 / TPAOH / Na_2O / H_2O=1.0 / 217 / 128 / 3.75 / 4496.The resulted powders were calcined at 550 ºC for 10h with a heating rate of 1 ºC /min to burn off the structure-directing agent TPAOH. The ZSM-5 crystals with the size of 100-200 nm were obtained.Then the prepared ZSM-5 was stirred in NaOH (0.2 M) for an hour at 90 ºC or 20s under microwave condition. The reaction was quenched by soaking in an ice-water bath to room temperature. The solid product was obtained by centrifugation and dried at 100 ºC.Then we used gel-casting method to obtain the macroporous precursor. Organic monomer acrylamide (AM) was dissolved in the water, crosslinker N, N-methylenebisacrylamide (MBAM) was added with stirring for 30 minutes, then the prepared ZSM-5 with hollow structure was added into the solution with strong agitation for 36 hours, followed by adding initiator ammonium persulfate. The composition weight ratio is ((5–10) AM/(0.05–0.1) MBAM/(0.01–0.025) $(NH_4)_2S_2O_8$/(90–95) silicalite solid. Until a homogeneous solution was obtained, the whole suspension was ultra-sonicated for 5–10 minutes to ensure good homogeneity. The gel-casting of the resulting colloidal suspension was carried out in a home-made mold (Centrifuge tube), sealed statically at 60 ºC for 6 hours until the organic monomer in the suspension were polymerized, then dried at 60 ºC for 2–3 days and further dried at 100 ºC overnight. Before drying, the suspension-filled mold was hand-shaken for a few minutes to release air bubbles. After drying, the tubular gel-casting sample was sintered under air at a heating rate of 1 ºC/ min up to 500 ºC, and kept it for 8 h to burn off the organic polymer, for sintering together the silicalite nanocrystals through condensation cross-linking of the surface silanol groups of nanocrystals.[40-41] The fabrication process of G-ZSM-5 was illustrated in Figure 8. Since the suspension with monomer, crosslinker, and initiator had low viscosity and good fluidity, it can be easily transferred into the mold.[24] Once the temperature increased to 60 ° C, the monomers in the suspension were quickly polymerized and crosslinked freeradically into an elastic hydrogel.[42-44] A highly crosslinked polyacrylamide hydrogel obtained was expected to link with silicalite nanocrystals because of the interaction of the surface silanol groups and -NH_2 groups. The solidified suspension (a gel-cast) was mechanically strong and easily removed from the mold.

3. Characterizations.

X-ray diffraction (XRD) patterns were obtained with a Rigaku D/Max-2550 diffractometer using Cu Kα radiation (λ= 1.5418 Å) operated at 50 kV and 200 mA with the 2θ scanning speed of 10 (°)/min between 4°and 40°. Scanning electron microscopy (SEM) was performed on a Hitachi JSM-6700F field emission scanning electron microscope with an accelerating voltage of 50 KV. Transmission electron microscopy (TEM) images were recorded on a JEOL JSM-2010F field emission transmission electron microscope operated at 300 kV. The nitrogen isotherms were measured on a Micromeritics ASAP 2010 sorptometer at 77K. The samples were degassed at 200 ºC for 8 h before measurement to desorb moisture adsorbed on the surface and inside the porous networks. Surface areas and pore structures were achieved from Brunauer–Emmett–Teller (BET) method. The pore-size distribution for mesopores was calculated by using the Barrett-Joyner-Halenda (BJH) model.[45]

Adsorption and desorption isotherms for Ar at 87.3 K were recorded with a Micromeritics ASAP 2010 sorptometer. Before measure, sample was out gassed at 573 for 6 h. The micropore volume were derived preferably using the t-plot (N_2 and Ar) methods, while the mesopore volume were derived by the external surface area by the t-plot. The catalytic cracking reactions of Hexane was carried out according to the following conditions: mass of the catalyst was 0.05 g with 20-40 mesh; reaction temperature was under temperature 400℃ (no thermal cracking); and the ratio of Hexane to the catalyst was 0.4 μL/0.05 g. Nitrogen was used as the carrier gas at a flow rate of 83mL/min, under the atmospheric pressure of 0.1MPa. Differential thermal analysis (DTA) and thermogravimetric analysis (TG) were performed on NETZSCH STA 449C between room temperature and 800℃ at a rising rate of 10℃/min. The Si/Al molar ratio of samples were determined by induced coupled plasma emission spectrum analyzer (ICP). Temperature-programmed-desorption of ammonia (TPD-NH_3) curves were recorded on automated chemisorption (Micromeritics AutoChem II 2920) in the range 100-800 ºC with a temperature-increasing rate of 10 ºC/min. Fourier Transform Infrared Spectroscopy were performed on a Bruker IFS 66 V/S FTIR spectrometer. The ratio of sample to KBr was 1/50, scan time was 32s.

4. Catalytic Reactions.

Two catalytic reactions were used to evaluate catalytic performance of the G-ZSM-5 materials, and analyses of the catalytic products were carried out with pulse chromatography (SHIMADZU GC-14C gas chromatographs equipped with FID detectors). Samples were treated with 2 M NH_4NO_3 for 3h, filtered and dried for 8 h under 80 ºC, then calcined at 550 ºC for 5 h to burn off residual organic templates and protonated for several times. Catalytic cracking reactions of 1, 3, 5- triisopropylbenzene were used to evaluate catalytic performance of the hierarchical ZSM-5 materials. Comparing with precursor ZSM-5, we found the product treated with gel-casting method (G-ZSM-5) performed better catalytic activity. Catalytic cracking of n-hexadecane was used to evaluate catalytic performance of the hierarchical ZSM-5 materials, comparing with P-ZSM-5, traditional Beta, Al-MCM-41 and SBA-15, and we found the product treated with gel-casting method (G-ZSM-5) performed better Catalytic activity. The catalytic measurement was carried out according to the following conditions: mass of the catalyst was 0.025 g with 20-40 mesh; reaction temperature was under temperature 250 ºC, 280 ºC,320 ºC, and 360 ºC (no thermal cracking); and the ratio of n-hexadecane to the catalyst was 0.1 μL/0.025 g. Nitrogen was used as the carrier gas at a flow rate of 48 mL/min, under the atmospheric pressure of 0.1MPa. The catalytic cracking reactions of 1,3,5-triisopropylbenzene was carried out according to the following conditions: mass of the catalyst was 0.05 g with 20-40 mesh; reaction temperature was under temperature 200℃, 250℃, and 320 ℃ (no thermal cracking); and the ratio of 1,3,5-triisopropylbenzene to the catalyst was 0.4 μL/0.05 g. Nitrogen was used as the carrier gas at a flow rate of 48mL/min, under the atmospheric pressure of 0.1MPa.[46-47]

Acknowledgements.

View Article Online
DOI: 10.1039/C5NJ03387J

This work is supported by the National Science Foundation Project of China (21390394, 91022030 and 20971052), and the New Century Outstanding Scholar Supporting Program.

Notes and references

1.H. Manzano, L. Gartzia-Rivero, J. Bañuelos and I. López-Arbeloa, *J. Phys. Chem. C*, 2013, **117**, 13331; M. Veiga-Gutiérrez, M. Woerdemann, E. Prasetyanto, C. Denz and L. De Cola, *Adv. Mater.*, 2012, **24**, 5199.
2.M. Hartmann, *Angew. Chem. Int. Ed.*, 2004, **43**, 5880.
3.J. Perez-Ramírez, C. H. Christensen, K. Egeblad, C. H. Christensen and J. C. Groen, *Chem. Soc. Rev.*, 2008, **37**, 2530.
4.I. L. C. Buurmans, J. Ruiz-Martínez, W. V. Knowles, D. van der Beek, J. A. Bergwerff, E. T. C. Vogt and B. M. Nat. Weckhuysen, *Chem*, 2011, **3**, 862.
5.S. Lopez-Orozco, A. Inayat, A. Schwab, T. Selvam and W. Schwieger, *Adv. Mater.*, 2011, **23**, 2602.
6.D. P. Serrano, J. M. Escola and P. Pizarro, *Chem. Soc. Rev.*, 2013, **42**, 4004.
7.W. J. Roth, P. Nachtigall, R. E. Morris and J. Č ejka, *Chem. Rev.*, 2014, **114**, 4807.
8.J. Cˇ ejka and S. Mintova, *Catal. Rev. Sci. Eng.*, 2007, **49**, 457; J. Qi, T. Zhao, F. Li, G. Sun, X. Xu, C. Miao, H. Wang and X. Zhang, *J. Porous Mater.*, 2010, **17**, 177; S. Bao, G. Liu, X. Zhang, L. Wang and Z. Mi, *Ind. Eng. Chem. Res.*, 2010, **49**, 3972; D. P. Serrano, J. Aguado, G. Morales, J. M. Rodriguez, A. Peral, M. Thommes, J. D. Epping and B. F. Chmelka, *Chem. Mater.*, 2009, **21**, 641.
9.Y. Zhu, Z. L. Hua, J. Zhou, L. J. Wang, J. J. Zhao, Y. Gong, W. Wu, M. L. Ruan and J. L. Shi, *Chem. -Eur. J.*, 2011, **17**,14618.
10.K. Egeblad, C. H. Christensen and M. Kustova, *Chem. Mater.*, 2008, **20**, 946.
11.J. Pérez-Ramírez, C. H. Christensen, K. Egeblad, C. H. Christensen and J. C. Groen, *Chem. Soc. Rev.,* 2008, **37**, 2530.
12.D. P. Serrano, J. M. Escola and P. Pizarro, *Chem. Soc. Rev.,* 2013, **42**, 4004.
13.S. Mintova, J. P. Gilson and V. V., *Nanoscale*, 2013, **5**, 6693.
14.S. Mitchell, A. B. Pinar, J. Kenvin, P. Crivelli, J. Kärger and J. P. Ramírez, *Nat. Commun.,* 2015, **6**:8633
15.P. B. Weisz and J. S. Hicks, *Chem. Engng. Sci.*, 1962,.**17**,265.
16.Roberta Bigliani *IDC Energy Insights*. 2013, **5.**
17.G. Onyestyák, J. Valyon and K. Papp, *Mater. Sci. Eng.*, A 2005, **412**, 48.
18.M. Choi, K. Na, J. Kim, Y. Sakamoto, O. Terasaki and R. Ryoo, *Nature*, 2009, **461**, 246.
19.B. Louis, F. Ocampo, H. S. Yun, J. P. Tessonnier and M. M. Pereira, *Chem. Eng. J.*, 2010, **161**, 397.
20.L. Xu, S. J. Wu, J. Q. Guan, H. S. Wang, Y. Y. Ma, K. Song, H. Y. Xu, H. J. Xing, C. Xu, Z. Q. Wang and Q. B. Kan, *Catal. Commun.* 2008, **9**, 1272.
21.M. Rauscher, T. Selvam, W. Schwieger and D. Freude, *Microporous Mesoporous Mater.*, 2004, **75**, 195.
22.M. Ogura, S. Y. Shinomiya, J.Tateno, Y. Nara, M. Nomura and E. Kikuchi, *Appl. Catal.*, A 2001, **219**, 33.
23.H. B. Zhu, Z. C. Liu, D. J. Kong, Y. D. Wang, X. H.Yuan and Z. K. Xie, *J. Colloid Interface Sci.*, 2009, **331**, 432.
24.Q. F. Tan, X. J. Bao, T. C. Song, Y. Fan, G. Shi, B. J. Shen, C. H. Liu and X. H. Gao, *J. Catal.*, 2007, **251**, 69.

View Article Online
DOI: 10.1039/C5NJ03387J

25.B. Louis, C. Tezel, L. Kiwi-Minsker and A. Renken, *Catal. Today.*,2001, **69**, 365.
26.J. Čejka and S. Mintova, *Catal. Rev.*, 2007, **49**, 457.
27.A. H. Janssen, I. Schmidt, C. J. H. Jacobsen, A. J. Koster and K. P. de Jong, *Microporous Mesoporous Mater.*, 2003, **65**, 59.
28.D. J. Wang, Z. N. Liu, H.Wang, Z. K. Xie and, Y. Tang, *Microporous Mesoporous Mater.* ,2010, **132**, 428.
29.S. Mitchell, N. Michels, J. Perezramirez, *Chem. Soc. Rev.,* 2013, **42**, 6094
30.J. S. J. Hargreaves, A. L. Munnoch, *Catal. Sci. Technol.,* 2013, **3**, 1165
31.Z. T. Zhang, Y. Han, F. S. Xiao, S. L. Qiu, L. Zhu, R. W. Wang, Y. Yu, Z. Zhang, B. S. Zou, Y. Q. Wang, H. P. Sun, D. Y. Zhao and Y. Wei, *J. Am. Chem. Soc.,* 2001, **21**, 5015.
32.C. Young, O. O. Omatete, M. A. Janney and P. A. Menchhofer, *J. Am. Ceram. Soc.*, 1991, **74**, 612.
33.H. T. Wang, X. Q. Liu, H. Zheng, W. J. Zheng and G. Y. Meng, *Ceram. Int.*, 1999, **25**, 177.
34. H. T. Wang, L. M. Huang, Z. B. Wang, A. Mitra and Y. S. Yan, *Chem. Commun.*, 2001, 1364.
35.Y. J. Jiang, K. Zhang, T. S.Zhao , X. J. Yong, C. T. Luo, *Chemical Reaction Engineering and Technology*, 2014, **06**, 0528.
36.J. M. Chen, P. Tan, J. Y. Wang, *Powder Metallurgy Industry,* 2011, **2**, 21.
37.Z. T. Zhang, X. H. Gao, D. O. Xu, L. J. Yan, R. W. Wang, Z. Y. Zhou, *CN. Patent CN201110070493*. **2.** 2011
38.L. M. Huang, Z. B. Wang, J. Y. Sun, L. Miao, Q. Z. Li, Y. Yan and D. Y. Zhao, *J. Am. Chem. Soc.*, 2000, **122**, 3530.
39.H. T. Wang, Z. B. Wang and Y. Yan, *Chem. Commun.*, 2000, **23**, 2333.
40.H. B. Zou, R. W. Wang, X. X. Li, X. Wang, S. J. Zeng, S. Ding, L. Li, Z. T. Zhang and S. L. Qiu, *J. Mater. Chem.* A, 2014, **2**, 12403
41.T. Xiao, L. An and H. Wang, *Appl. Catal., A*, 1995, **130,** 187.
42.J. J. Zheng, X. W. Zhang, Y. Zhang, J. H. Ma and R. F. Li, *Microporous Mesoporous Mater.*, 2009, **122**, 264.
43.S. Abelló, A. Bonilla and J. Pérez-Ramírez, *Appl. Catal.*, A 2009, **364**,191.
44.H. T. Wang, L. M. Huang, Z. B. Wang, A. Mitra and Y. S. Yan, *Chem. Commun.*, 2001,**15**, 1364.
45.Z. T. Zhang, Y. Han, L. Zhu, R. W. Wang, Y. Yu, S. L. Qiu, D. Y. Zhao, and F. S. Xiao, *Angew. Chem. Int. Ed.* 2001, **40,** 7.
46.J. Qi, T. B. Zhao, X. Xu, F. Y. Li, G. D. Sun，Physicochemical Properties and Catalytic Technology,2010, 12, 17-22.
47.J. H. Li, D. Zhang, X. Li, Chinese journal of inorganic chemistry, 2004. 29, 2049.

View Article Online
DOI: 10.1039/C5NJ03387J

3D hierarchical porous ZSM-5 zeolite as a catalytic material for the cracking of n-hexadecane is reported.